Journal of Atmospheric and Solar–Terrestrial Physics 198 (2020) 105180

Contents lists available at ScienceDirect

Journal of Atmospheric and Solar-Terrestrial Physics

journal homepage: www.elsevier.com/locate/jastp

Research Paper

Characterization of optically effective complex refractive index of black carbon composite aerosols

Xiaolin Zhang [a,b,c,d], Mao Mao [a,c,*], Hongbin Chen [b]

[a] Key Laboratory of Meteorological Disaster, Ministry of Education (KLME), Collaborative Innovation Center on Forecast and Evaluation of Meteorological Disasters (CIC-FEMD), Joint International Research Laboratory of Climate and Environment Change (ILCEC), Earth System Modeling Center (ESMC), Key Laboratory for Aerosol-Cloud-Precipitation of China Meteorological Administration, Nanjing University of Information Science & Technology, Nanjing 210044, China

[b] Key Laboratory of Middle Atmosphere and Global Environment Observation (LAGEO), Institute of Atmospheric Physics, Chinese Academy of Sciences, Beijing 100029, China

[c] School of Atmospheric Physics, Nanjing University of Information Science & Technology, Nanjing 210044, China

[d] National Satellite Meteorological Center, China Meteorological Administration, Beijing 100081, China

ARTICLE INFO

Keywords:
Aerosol
Optically effective complex refractive index
Aerosol-climate model
Numerical retrieval

ABSTRACT

Black carbon aerosols, always existing as complicated mixtures of various species, have important impacts on the global and regional climate, whereas their effective aerosol complex refractive index (ACRI) is a must for modeling their radiative effects. Retrieval of optically effective ACRI from accurately calculated scattering and absorption properties of an internal-mixed aerosol model with BC and dust coated with sulfate, roughly representing ambient aged multicomponent BC particles, are performed. The sensitivities of retrieved optically effective ACRI to particle size distribution and composition ratio are explored, and the popular volume weighted average (VWA) method and Bruggeman effective medium (BEM) theory are also considered for comparison. The optically effective ACRIs depicts dramatic variation for monodisperse size parameter larger than π, as opposed to almost a constant for size parameter less than π, whereas the VWA and BEM can hardly provide acceptable effective ACRIs for coarse BC composite particles. The retrieved optically effective ACRI are sensitive to both size distribution and composition ratio, and becomes more sensitive to particle size distribution with aerosols containing more BC content. As BC volume content reaches ~4%, the VWA overestimates the imaginary part of effective ACRI with significant bias when compared with the optically effective ACRI, indicating overestimated aerosol absorption in most atmospheric environments in aerosol-climate models employing the VWA. We suggest that the optically effective ACRI, rather than the ACRI given by the VWA, should be applied to account for coarse BC-containing particles in the state-of-the-art aerosol-climate models.

1. Introduction

Aerosols in the atmosphere can affect globe and regional climate directly by scattering and absorbing solar radiation, and indirectly by modifying cloud properties as condensation nuclei (IPCC, 2013). The absorptive black carbon (BC) aerosols have positive warming radiative forcing second to CO_2, making it an important near-term climate mitigation target (Grieshop et al., 2009; Shindell et al., 2012). Quantitative prediction of ambient BC aerosol climate effects is challenging, and one of the reasons is that BC aerosols always exist as complicated mixtures of various species in ambient air (e.g., Bellouin, 2014; Saleh et al., 2014). The largest uncertainty in the estimation of aerosol effects on climate roots in uncertainties in determining their microphysical properties, including the aerosol complex refractive index (ACRI), which in turn determines their radiative properties, and these uncertainties can be related to effective emissions, spatial distributions of sources and temporal variability of emissions.

The ACRI, a pivotal parameter governing particle inherent scattering and absorption properties, should be known for modeling the radiative effects of aerosols. The magnitude of radiative forcing is very sensitive to

* Corresponding author. Key Laboratory of Meteorological Disaster, Ministry of Education (KLME), Collaborative Innovation Center on Forecast and Evaluation of Meteorological Disasters (CIC-FEMD), Joint International Research Laboratory of Climate and Environment Change (ILCEC), Earth System Modeling Center (ESMC), Key Laboratory for Aerosol-Cloud-Precipitation of China Meteorological Administration, Nanjing University of Information Science & Technology, Nanjing 210044, China.

E-mail address: mmao@nuist.edu.cn (M. Mao).

https://doi.org/10.1016/j.jastp.2019.105180
Received 28 August 2019; Received in revised form 4 December 2019; Accepted 6 December 2019
Available online 10 December 2019

ACRI, and the dependence of radiative forcing on its imaginary part is even more pronounced than that on real part (Raut and Chazette, 2008a). Accurate determining ACRI, especially the imaginary part, is consequently essential for deducing optical properties and then aerosol effects on climate. However, ambient aerosols are generally complex mixtures of different species, and it is not feasible to calculate aerosol radiative properties based on refractive indices of all compositions of each individual particle within an aerosol population. An effective ACRI of complex-mixed particles is therefore normally used to represent the whole size distribution (Redemann et al., 2000; Guyon et al., 2003). The effective ACRI might generally include the chemically effective ACRI and optically effective ACRI on the basis of derived methods. The determination of chemically effective ACRI is often provided from bulk chemical compositions and known values of the refractive indices of pure components (e.g., Kandler et al., 2009). Whereas, the optically effective ACRI of a mixture is retrieved from its inherent optical properties, and might produces the same (or very similar) optical properties as the inherent values under the same particle shapes.

The volume weighted average (VWA) method is one method applied to determine the chemically effective ACRI, and the choice of this approach is driven by high dependency of ACRI on aerosol chemical compositions (Chazette and Liousse, 2001; Kandler et al., 2009). For instance, Marley et al. (2001) obtain preliminary ACRI results for carbon soot samples generated in the laboratory and for standard diesel soot samples in the UV/visible spectral range. This traditional VWA method is also widely utilized in the state-of-the-art aerosol-climate models, approximating effective ACRIs of internal- and external-mixed aerosol ensemble at each mode for calculating their radiative properties (e.g., Stier et al., 2005). However, the performance of the VWA approximation is still an open question. Besides the VWA, the effective medium theory (EMT) is the other method for the determination of the chemically effective ACRI, and one of the most commonly applied EMTs is the Bruggeman theory (Bruggeman, 1935). In EMTs, the effective ACRI is determined from the effective dielectric constant derived firstly, and then optical properties of heterogeneous scatter are approximated by those of a homogeneous particle of the same shape. The EMT is extensively used in many previous researches (e.g., Abo Riziq et al., 2007; Mishchenko et al., 2016), while several studies have questioned the validity of the EMT due to the possible significant errors depending on the particles in question (e.g., Saija et al., 2003; Voshchinnikov et al., 2007).

Besides the chemically effective ACRI, studies focusing on the determination of optically effective ACRI have been carried out. Dubovik et al. (2002b, 2006) apply a spheroidal dust model to derive ACRI from Sun photometer observations with AERONET (Aerosol Robotic Network) data. With the assumption of spherical particles and chemical homogeneity of aerosol samples, effective ACRI can be retrieved based on simultaneous measurements of size distributions, scattering and absorption coefficients (Riziq et al., 2007; Schkolnik et al., 2007; Mack et al., 2010; Stock et al., 2011). Raut and Chazette (2008a, 2008b) perform the retrieval of optically effective ACRI utilizing a synergy between lidar, sunphotometer and in situ measurements combined with a Mie theory based data analysis scheme. The retrieving techniques for effective ACRI using airborne in situ measurements of aerosol size distributions and absorption coefficients from a three-wavelength Particle Soot Absorption Photometer (PSAP) (Petzold et al., 2009) or Spectral Optical Absorption Photometer (SOAP) (Muller et al., 2009), have also been presented. Furthermore, Muller et al. (2010) compare derived ACRIs from different techniques and reveal only partly a reasonable agreement with distinct differences for the spectra of imaginary part remaining. As discussed above, significant retrievals of effective ACRI from measured ambient aerosol optical properties have been carried out, whereas theoretical investigation of the optically effective ACRI is missing. During the ACRI retrieval based on measured aerosol optical properties, uncertainties are caused due to instrumental errors and actual particle shapes (not all ambient aerosols are spherical or spheroidal particles). This significantly limits our ability to understand the relationship between aerosol microphysical properties, e.g., composition ratio and size distribution, and the optically effective ACRI retrieved from their optical properties, and to furthermore improve radiation simulations in aerosol-climate models. Therefore, a systematic numerical investigation on the optically effective ACRI is necessary and meaningful and will benefit the radiative transfer simulations, remote sensing applications and aerosol-climate model improvement.

As a result, a numerical investigation on the optically effective ACRI retrieved from accurately calculated scattering and absorption properties of composite black carbon aerosol are presented here. The effect of BC composition ratio and size distribution on retrieved optically effective ACRI, as well as its comparison with chemically effective ACRIs obtained from the VWA and EMT approximations are systematically stressed. The particle geometries simulated, accurate scattering calculation methods and retrieval approach are discussed in section 2. Section 3 illustrates the monodisperse and polydisperse results, and section 4 concludes the work.

2. Methodology: simulated model and retrieval approach

2.1. Aerosol model and scattering simulations

The freshly emitted soot is initially hydrophobic and mostly externally mixed with nonrefractory compounds and it becomes hydrophilic and more internally mixed with other aerosol species (such as dust) through condensation and coagulation with the time going (e.g., Guazzotti et al., 2001). Observations indicate that in polluted urban air, black carbon becomes internally mixed on a timescale of ~12 h with a coating of organics and sulfate (Moteki and Kondo, 2007; Shiraiwa et al., 2007) and becomes more spherical ones during the aging process (Smith and Grainger, 2014; Peng et al., 2016). Thus, this study considers a spherical internal-mixed aerosol model with the secondary sulfate coated on two inclusions which are an irregular dust and spherical BC (Fig. 1), which is generally similar to those applied in Shi et al. (2019). It should be noticed that we only focus on this simple but general example, and aerosol compositions in the model may be flexible enough to account for variation ranges of common refractive index.

Multiple numerical methods can be utilized to simulate inherent optical properties of aerosol particles, including the exact Mie method (Wiscombe, 1980) and discrete dipole approximation (DDA) (Draine

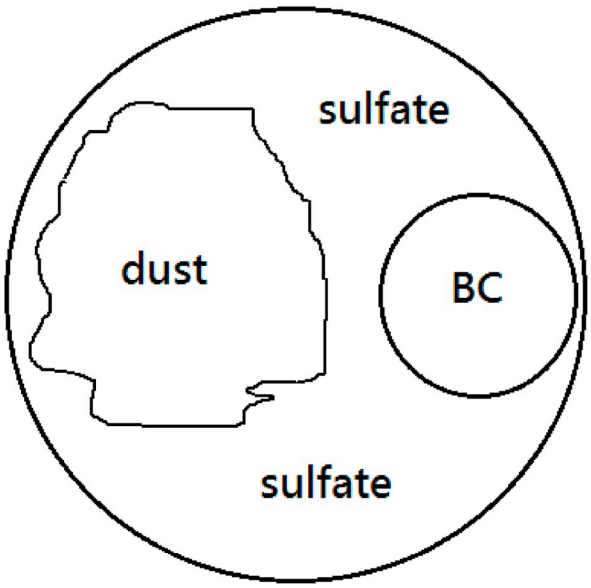

Fig. 1. Geometry of modelled internal-mixed aerosol particle. The internal mixture contains dust and black carbon (BC) coated by sulfate sphere.

and Flatau, 1994, 2008). The DDA method consists of approximating the actual target by an array of polarizable points and computes the incident-light interactions with these dipoles. This method provides accurate optical properties of arbitrary-shaped particles, rendering very accurate results for targets with size parameter not more than 25 (Flatau and Draine, 2012). The size parameter is defined as $\frac{2\pi r}{\lambda}$, where r is particle radius and λ is incident wavelength. The orientation-averaged optical properties of simulated BC composite internal mixture were computed based on the DDA method, whereas those of homogenous spherical particles are calculated using Mie method.

2.2. Retrieval approach

In our approach, the optically effective ACRI of internal-mixed particles is defined as an ACRI that provides almost the same scattering and absorption properties as their inherent properties, on the basis of known size distribution for homogeneous particles. The retrieval approach is similar to relevant methods described in previous studies (e.g., Mack et al., 2010; Stock et al., 2011; Zhang et al., 2013), with the differences lying in the inherent aerosol optical properties calculated accurately rather than measured and particle shapes not changed during retrieval. Among all aerosol optical properties, the scattering and absorption are chosen for retrieval, as both are basically governed by the real and imaginary part of ACRI, respectively.

The optically effective ACRI is determined by an iterative algorithm based on their size distributions and calculated scattering and absorption properties. Exploiting all calculations, the designed inversion scheme to retrieve the optically effective ACRI is as follows. Based on a guess for a real, n, and imaginary part, k, of the ACRI at a given wavelength, two look-up tables are built from the database using known size distribution. One look-up table contains the scattering cross sections and the other encompassed the absorption cross sections.

For physically-based sense, guessed real parts and imaginary parts of optically effective ACRI are within refractive index ranges of given compositions of simulated internal-mixed particles. In this study, three aerosol compositions of BC, dust, and sulfate are considered, and their corresponding refractive indices at incident wavelength of 550 nm are $1.85 - 0.71i$ (Bond and Bergstrom, 2006), $1.519 - 1.6 \times 10^{-3}i$ (Balkanski et al., 2007), and $1.52 - 5.0 \times 10^{-4}i$ (Aouizerats et al., 2010), respectively. Therefore in our calculation, the guessed real part of refractive index varies from 1.519 to 1.85 with an equidistant space of 0.001 and the imaginary part changes from 5.0×10^{-4} to 0.71 with a logarithmic interval of 0.005. Then the retrieval algorithm simultaneously varies n and k, and scans through all physically possible ACRI values within a chosen resolution until it minimizes χ^2:

$$\chi^2(n,k) = \frac{1}{N}\sum_{i=1}^{N}\left[\left(\frac{C_{sca,calculated}(n,k) - C_{sca,inherent}}{C_{sca,inherent}}\right)_i^2 + \left(\frac{C_{sca,calculated}(n,k) - C_{abs,inherent}}{C_{abs,inherent}}\right)_i^2\right] \quad (1)$$

where $C_{sca,inherent}$ and $C_{abs,inherent}$ are inherent scattering and absorption cross sections of simulated internal-mixed particles, $C_{sca,inherent}(n,k)$ and $C_{abs,inherent}(n,k)$ are calculated scattering and absorption cross sections using scanning refractive index, $\chi^2(n,k)$ produces the fractional difference of the calculated scattering and absorption cross sections relative to the inherent properties, and N is the number of calculations used in the retrieval. The $\chi^2(n,k)$ values for scattering plus absorption are minimized by optimizing initial guess ACRI values, yielding an optically effective ACRI at this wavelength. Since the absorption is primarily determined by the magnitude of k while the scattering is mainly governed by the magnitude of n, the minimization of $\chi^2(n,k)$ value should deduce a unique retrieval result of optically effective ACRI.

3. Results and discussion

3.1. Monodisperse study

The retrieval of optically effective ACRI of monodisperse internal-mixed particles is initially studied, although aerosols in the atmosphere are polydisperse in nature. The monodisperse particles are firstly considered for two reasons: (1) to study the behavior of optically effective ACRI at different size modes (i.e., nuclei, accumulation and coarse), and (2) because it is the fundament to do the polydisperse investigation, which will be discussed in latter subsections. Fig. 2 provides a case study of optically effective ACRI retrieved from scattering and absorption properties of monodisperse internal-mixed aerosols. These monodisperse aerosols have aforementioned three compositions with a fixed radius ratio of 1/2/3 (BC/dust/whole mixture) (see Fig. 1). The scattering and absorption inherent properties of the aerosol model, i.e., BC and dust coated by a sulfate sphere, are calculated by the DDA method. The effective ACRIs of the mixtures and introduced differences of scattering and absorption coefficients are shown in Fig. 2. The differences are relative errors of scattering and absorption properties induced by retrieved effective ACRIs compared to initial inherent properties. The retrieved ACRIs of internal-mixed aerosols are optically effective, since the relative errors for both scattering and absorption properties were within 1% (see Fig. 2, bottom row).

Fig. 2 clearly shows that the optically effective ACRI of a mixture is quite sensitive to its size parameter. As the monodisperse size grows, retrieved optically effective ACRI of the three-component mixture does not remain constant. This is different from the behavior of normal ACRI, which does not depend on the size of the material. When particle size parameter is larger than π, it is profound to find that strong oscillations are noticed for both real and imaginary parts of retrieved optically effective ACRIs. The reason still needs further investigation, since the shapes of the particles are not changed during the retrieval. However, the optically effective ACRIs have weak oscillations, as the size parameter becomes smaller than π, with almost a constant in nuclei mode (particle size less than 0.1 μm). In coarse mode (aerosol size larger than 1.0 μm), the real parts of derived optically effective ACRIs depict more pronounced oscillations than their corresponding imaginary parts. For the internal-mixed particles with the same volume ratio of 1/8/19 (BC/dust/sulfate), their mean optically effective ACRIs at 550 nm in nuclei, accumulation (0.1–1.0 μm), and coarse modes are $1.538 - 2.440 \times 10^{-2}i$, $1.555 - 2.293 \times 10^{-2}i$, and $1.709 - 7.030 \times 10^{-3}i$, respectively, at selected size parameters (see Fig. 2, top row).

To illustrate the effect of composition ratio of a mixture on its optically effective ACRI, Fig. 3 compares the results for fixed radius ratios of 1/2/3, 0.5/2/3, 0.25/2/3, 0.125/2/3 (BC/dust/whole mixture) with corresponding BC volume contents of ~4%, 0.5%, 0.06%, 0.007%, respectively. We reduce the BC content, as BC has a much larger ACRI than dust and sulfate, and assess the sensitivity of optically effective ACRI to particle size and composition ratio. Again, all optically effective ACRI results of monodisperse internal-mixed aerosols are illustrated as functions of size parameter. At different BC contents, the retrieved optically effective ACRIs depict similar patterns in nuclei and coarse modes, i.e., nearly a constant in nuclei mode and prominent oscillation in coarse mode. Nevertheless, in accumulation mode, the optically effective ACRIs have weaker oscillations, when BC contents of the mixture become smaller. As BC volume contents decrease from 4% to 0.007%, mean real parts of optically effective ACRIs decrease by 1.1%, 2.2% and 4.5%, as well as average imaginary parts decreasing by 96.4%, 96.1% and 86.6%, in nuclei, accumulation and coarse modes, respectively. With the decrease of BC contents, mean real parts decrease more along with imaginary parts decreasing less in coarse mode compared to nuclei and accumulation modes. The dependence of BC content on retrieval results, emphasizes its significance on retrieving the optically effective ACRI in urban air. Even if BC content is few (see Fig. 3g),

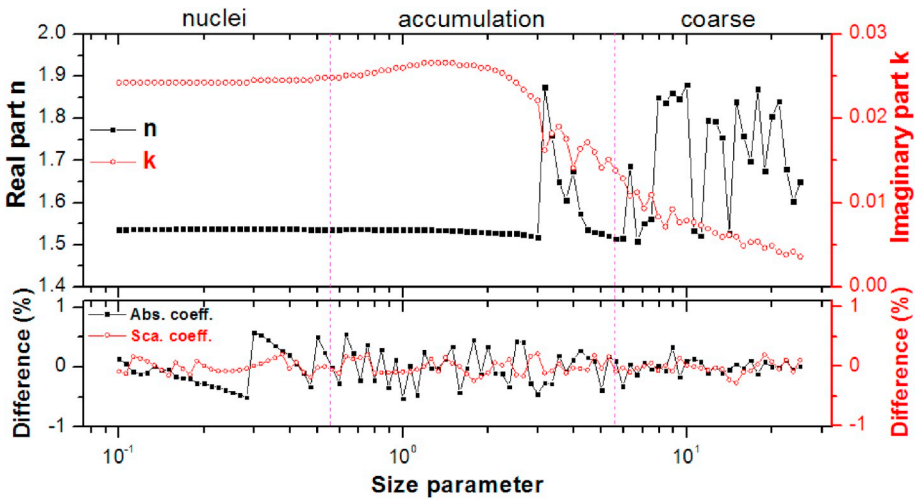

Fig. 2. The retrieved optically effective complex refractive indices (top row) of monodisperse internal-mixed particles with fixed radius ratio of 1/2/3 (BC/dust/whole sphere) and relative errors (bottom row) as a function of size parameter. For the aerosol complex refractive index (ACRI), the black solid squares denote the real part while the red open circles indicate the imaginary part. For the difference, the black solid squares and red open circles indicate the relative errors of absorption and scattering coefficients, respectively.

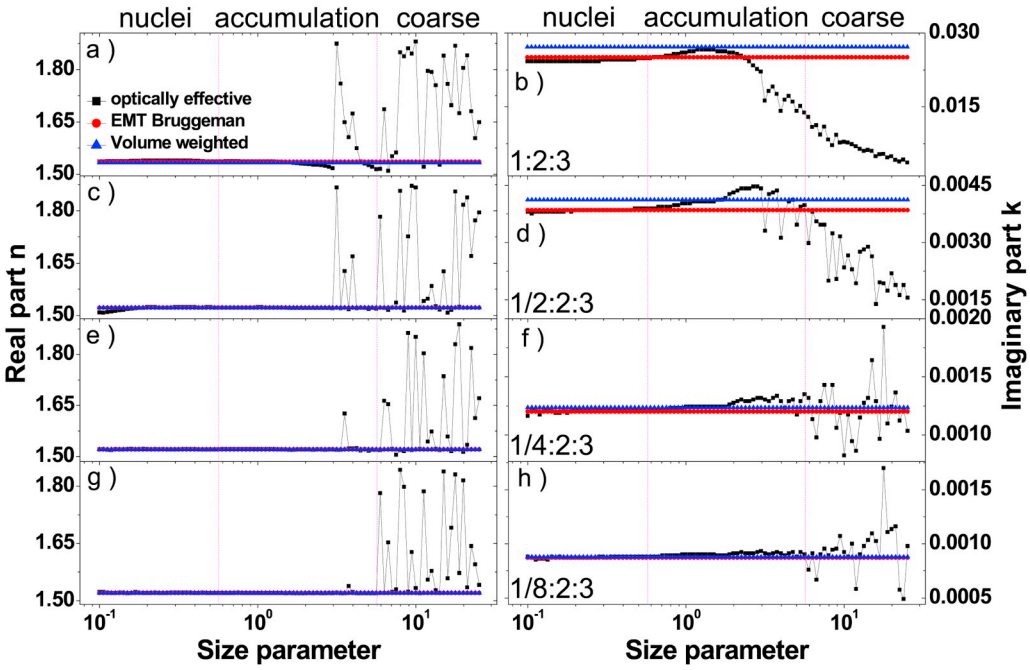

Fig. 3. The real parts (left four) and imaginary parts (right four) of retrieved complex refractive indices as a function of size parameter, for modelled monodisperse internal-mixed particles with fixed radius ratios (BC/dust/whole sphere) of (a, b) 1/2/3, (c, d) 0.5/2/3, (e, f) 0.25/2/3 and (g, h) 0.125/2/3, respectively. The black squares denote the optically effective ACRIs, whereas red circles and blue triangles indicate the retrieved ACRIs based on Bruggeman effective medium theory and volume weighted average method, respectively.

retrieved optically effective ACRI exhibits flattering eminent oscillations in coarse mode, indicating the complexity in knowing the optically effective ACRI for large internal-mixed particles. In brief, retrieved optically effective ACRIs of internal-mixed monodisperse particles portray approximately constant for size parameters less than π, as opposed to dramatic oscillations for size parameters larger than π. Meanwhile, the optically effective ACRIs of BC-dust-sulfate internal mixtures depict weaker oscillations with less BC content only in accumulation mode.

3.2. *Comparison with the volume weighted average and effective medium theory*

Besides the optically effective ACRI, another approaches to determine the effective refractive index of an internal-mixed particle are based on the chemically effective ACRIs, including the effective medium theory and the VWA method. The results of the VWV method, which is popularly utilized in the state-of-the-art aerosol-climate models, and the Bruggeman effective medium (BEM) theory are considered for comparison with the optically effective ACRI. With the fixed volume fractions and refractive indices of aerosol compositions, it is straight to calculate the chemically effective ACRIs.

The comparison of effective ACRIs employing these three different approaches for monodisperse BC-dust-sulfate internal-mixed particles is illustrated in Fig. 3. Considering that volume fractions of each composition are fixed, results of effective ACRIs based on the BEM and VWA methods are expressed by the horizontal symbol lines in the figure. The lower real parts as well as higher imaginary parts of the effective ACRIs produced by the VWA are obtained compared to the BEM. The effective ACRIs given by the BEM and VWA are mainly close to the optically effective ACRIs for particle size parameters less than π, whereas large differences exist for size parameters larger than π. With the decrease of BC content, the differences between the effective ACRIs given by the BEM and VWA and the optically effective ACRIs decrease averagely. For

a BC volume content reaching ~4%, when size parameter is less than π, relative differences of the real and imaginary parts of chemically effective ACRIs (given by the BEM and VWA) compared with optically effective ACRIs are within 0.2% and 8.8%, respectively. Meanwhile, with size parameter exceeding π, real parts of chemically effective ACRIs are on average ~9% larger than that of optically effective ACRIs, whereas the BEM and VWA overestimate imaginary parts medially by up to a factor of ~2 (see Fig. 3a and b). Even if BC volume content is as low as 0.007%, significant bias of an average ~7% is noticed in coarse mode for effective ACRIs computed by the BEM and VWA in comparison with optically effective ACRIs (see Fig. 3g and h). Generally, the VWA (and BEM) approximations, which show acceptable performance for effective ACRIs of internal-mixed particles in nuclei and small accumulation modes (size parameter <π), can hardly provide accurate results in coarse mode. Thus, the optically effective ACRI, instead of the effective ACRI given by the VWA, may have to be considered for coarse internal-mixed particles in aerosol-climate models.

3.3. Polydisperse study

Previous figures depict the optically effective ACRIs for monodisperse BC-dust-sulfate internal-mixed particles, while polydisperse results are discussed in following subsections. For ambient atmosphere, only the polydisperse bulk aerosol properties averaged over a certain size distribution are meaningful, although monodisperse particles can be used to examine the effective-ACRI patterns in different size modes. For polydisperse study, the radius of the internal-mixed particles are assumed to follow a lognormal size distribution (Stier et al., 2005) in the form of

$$n(\ln r) = \frac{1}{\sqrt{2\pi}\ln(\sigma_g)} \exp\left[-\left(\frac{\ln(r) - \ln(r_g)}{\sqrt{2}\ln(\sigma_g)} \right)^2 \right], \quad (3)$$

where r_g is the geometric mean radius, and σ_g is the geometric standard deviation.

Table 1 compares the bulk optically effective ACRIs of BC-dust-sulfate internal-mixed particles with different BC content at 550 nm wavelength. Again, the inherent aerosol properties for retrieval of optically effective ACRI are computed based on the DDA method. The bulk chemically effective ACRIs given by the BEM and VWA and corresponding induced differences of scattering and absorption cross sections are also listed in Table 1. A lognormal size distribution with a geometric mean radius of 0.05 μm and a standard deviation of 2.5 is assumed as a case study (Alexander et al., 2013). With the bulk scattering and absorption properties are averaged over different particle sizes, it should be expected that retrieved optically effective ACRIs are smoothed out. The real parts of polydisperse optically effective ACRIs are close to those produced by the BEM and VWA with differences typically negligible (within 1%). However, as BC volume content is ~4%, significant bias of ~10% is noticed for imaginary parts of optically effective ACRIs in comparison with those given by the VWA, resulting in that the VWA overestimates the absorption by over 50%. The large errors of aerosol scattering and absorption induced by the chemically effective ACRIs show the limitations of the BEM and VWA methods, which are only the simple approximations to obtain an effective refractive index for calculating aerosol optical and radiation properties easily and rapidly.

As listed in Table 1, retrieved optically effective ACRIs of polydisperse internal mixtures decrease with BC content decreasing. This is not amazing given that BC has high refractive index while dust and sulfate have similar and low refractive index. When BC volume contents decrease from ~4% to 0.007%, the real parts decrease by only 1% whereas the imaginary parts decrease by over 96%, indicating the effect of BC content on retrieved optically effective ACRI. With reduced BC contents, the effective ACRIs produced by the BEM and VWA are generally close to the optically effective ACRIs, especially the real parts.

Table 1
Summary of retrieved complex refractive indices of polydisperse particles with a lognormal distribution ($r_g = 0.05$, $\sigma_g = 2.5$).

Composition radius ratio[a]	ACRI	n[b]	k[c]	C_{sca} difference[d]	C_{abs} difference[e]
1:2:3	OE[f]	1.533	2.483×10^{-2}	−0.078%	0.500%
	EMT[g]	1.535	2.506×10^{-2}	−6.113%	50.367%
	VWA[h]	1.532	2.713×10^{-2}	−7.534%	58.635%
1/2:2:3	OE	1.521	4.027×10^{-3}	−0.109%	0.538%
	EMT	1.522	3.849×10^{-3}	0.325%	9.365%
	VWA	1.521	4.121×10^{-3}	−0.606%	16.390%
1/4:2:3	OE	1.520	1.230×10^{-3}	0.007%	−0.351%
	EMT	1.520	1.200×10^{-3}	−0.030%	−7.002%
	VWA	1.520	1.234×10^{-3}	−0.064%	−4.470%
1/8:2:3	OE	1.520	8.913×10^{-4}	0.059%	−0.095%
	EMT	1.520	8.722×10^{-4}	−0.069%	−7.252%
	VWA	1.520	8.763×10^{-4}	−0.070%	−6.811%

[a] Composition radius ratio given as BC/dust/whole sphere.
[b] Real part of retrieved aerosol complex refractive index.
[c] Imaginary part of retrieved aerosol complex refractive index.
[d] Relative error of scattering coefficient induced by retrieved refractive index with respect to inherent scattering.
[e] Relative error of absorption coefficient induced by retrieved refractive index with respect to inherent absorption.
[f] Aerosol optically effective complex refractive index.
[g] Aerosol effective complex refractive index based on Bruggeman effective medium theory.
[h] Aerosol effective complex refractive index based on volume weighted average method.

For a BC volume content of 0.007%, the relative differences of the real parts between them are few, and differences of the imaginary parts are ~2%, leading to a bias of aerosol absorption up to ~7%. In conclusion, for polydisperse BC-dust-sulfate internal-mixed particles with a whole size distribution, i.e., from nuclei to coarse mode, the BEM and VWA approximations provide acceptable performance only for low BC contents. When BC volume content reaches ~4%, significant errors of the imaginary parts (over 10%) would be introduced if the BEM and VWA are utilized. This will generate more biases in optical properties of aerosols, definitely inducing shifty influences on their interactions with the solar radiation, which will be investigated in further studies.

3.4. Effect of size distribution on optically effective refractive index

Fig. 4 illustrates retrieved optically effective ACRIs with different size distribution, and the panels from left to right correspond to two cases with aforementioned fixed radius ratio of 1/2/3 and 0.125/2/3 (BC/dust/whole sphere), respectively. The lognormal size distributions are assumed for the BC-dust-sulfate internal-mixed particles with r_g (x axis) ranging from 0.05 μm to 1.0 μm and σ_g (y axis) ranging from 1.1 to 2.5. Fig. 4 clearly portrays that the optically effective ACRI is quite sensitive to both particle size distribution and composition ratio. For BC-dust-sulfate aerosols with a BC volume content of ~4% (see Fig. 4a and b), the real parts of optically effective ACRIs are in a range between 1.520 and 1.539, whereas the imaginary parts vary twofold ranging from 1.16×10^{-2} to 2.63×10^{-2}. As depicted in Fig. 4a, the real parts of optically effective ACRIs generally decreases as r_g or σ_g increases, i.e., particle becoming larger or size distribution becoming wider. The

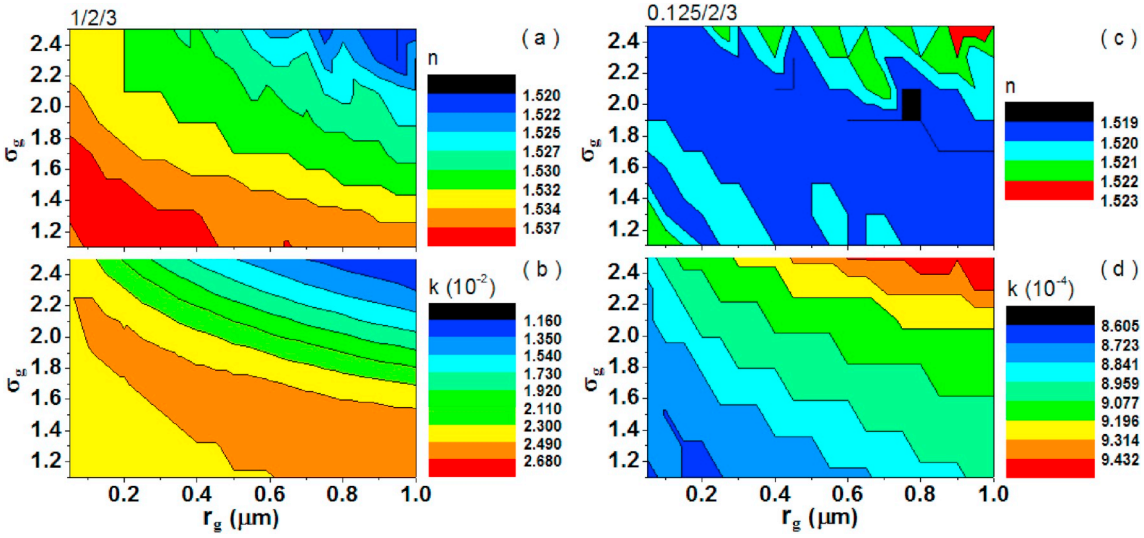

Fig. 4. The retrieved optically effective complex refractive indices of polydisperse internal-mixed particles with fixed radius ratio of (left two) 1/2/3 and (right two) 0.125/2/3 (BC/dust/whole sphere), respectively, for different lognormal size distributions. Top two (a, c) indicate the real part, while bottom two (b, d) denote the imaginary part.

unsmooth variation of the polydisperse real parts can be explained based on aforementioned monodisperse results, showing that the real parts for large particles are oscillating with size variation. In Fig. 4b, the imaginary parts show similar patterns to those of the real part, whereas the variations on size distribution are more complicated. For a diminished BC volume content as few as 0.007% (see Fig. 4c and d), the real and imaginary parts of retrieved polydisperse optically effective ACRIs have narrow ranges of 1.519–1.523, and 8.61×10^{-4} – 9.55×10^{-4}, respectively. The retrieved real parts show weak variation on particle size distribution, while the imaginary parts depict almost opposite patterns to those in the case with BC content reaching ~4%. Comparing the results of both composition ratios, the optically effective ACRI becomes more sensitive to the size distribution, i.e., showing larger variation, as internal-mixed aerosol particles have more BC content.

For the BEM and VWA approximations, the effective ACRIs are constant values, as each polydisperse internal-mixed particles have fixed composition ratios. For BC volume contents of ~4% and 0.007%, the effective ACRIs given by the BEM are $1.535 - 2.51 \times 10^{-2}i$ and $1.520 - 8.72 \times 10^{-4}i$, whereas the values given by the VMA are $1.532 - 2.71 \times 10^{-2}i$ and $1.520 - 8.76 \times 10^{-4}i$, respectively. The relative differences between the real parts produced by the BEM and VWA and optically effective ACRIs are under 1% for BC contents of both ~4% and 0.007%. Nevertheless, important bias is noticed for the imaginary part with relative differences even over 100% at particle size distributions having large r_g and σ_g, when the BC content reaches 4%. For internal-mixed particles having few BC content of 0.007%, an imaginary-part difference of ~10% could be introduced by the BEM and VWA compared to optically effective ACRIs at size distributions with large r_g and σ_g, although it is relatively small for most size distributions. The imaginary parts given by the VWA are larger than those of optically effective ACRIs for BC content reaching 4%, whereas the reverse is generally true for BC content as low as 0.007%. This may be partly attributed to the lensing effect (e.g., Cappa et al., 2012; Liu et al., 2015; Zhang et al., 2017, 2018), which describes enhanced light absorption of BC coated with non-BC species, since the imaginary part of refractive index is mainly associated with aerosol absorption. The BC internal-mixed particles with few BC content have prominently large absorption enhancements, resulting in a relatively 'high' optically effective imaginary part, which is generally larger than the VWA result. On the contrary, the aerosols containing more BC content show comparatively smaller absorption enhancements, so that the imaginary part of optically effective ACRI lower than the VWA result is observed. Overall, the optically effective ACRI is both sensitive to composition ratio and size distribution, and the sensitivity of the optically effective ACRI to size distribution becomes stronger as particle has more BC content. With a BC volume content reaching ~4%, the VWA approximation overestimates the imaginary part of effective ACRI with significant bias when compared with the results of optically effective ACRI. This suggests that aerosol absorption may be overestimated in most atmospheric environments in climate models, which is probably one of the reasons why modelled aerosol optical depth is 20% larger than observed (Roelofs et al., 2010), since the VWA approximation is applied in the state-of-the-art aerosol-climate models.

4. Conclusions

The study explores the impacts of size distribution and composition ratio on retrieved optically effective ACRI of BC composite aerosol. The internal-mixed aerosol model with BC and dust coated with sulfate is roughly applied to simulate aged multicomponent BC particles. Our results indicate that both size distribution and composition ratio have significant effects on retrieved optically effective ACRI of BC-dust-sulfate internal-mixed aerosols. The optically effective ACRIs depicts dramatic variation for monodisperse size parameter larger than π, as opposed to nearly a constant for size parameter less than π. Meanwhile, reducing BC content cannot smooth out intense variation of optically effective ACRIs in coarse particle mode, despite their mean values decreasing. The VWA (and BEM) can hardly produce acceptable effective ACRIs in coarse mode, even if their BC content is few, and thus, the optically effective ACRI should be used to account for coarse BC composite particles in aerosol-climate models.

When aerosols contain more BC content, the sensitivity of retrieved optically effective ACRI to particle size distribution becomes stronger. With a BC volume content reaching ~4%, the VWA overestimates the imaginary part of effective ACRI with significant bias in comparison with results of optically effective ACRI, suggesting overestimated aerosol absorption in most atmospheric environments in the state-of-the-art aerosol-climate models employing the VWA. This may be one of the reasons why aerosol optical depth modelled by the aerosol-climate model is 20% larger than observed (Roelofs et al., 2010). Although some flattering results are profound to be found in the study, the conclusions given should be carefully verified before being applied for other cases due to retrieved optically effective ACRIs being highly complicated functions of aerosol microphysical properties (such as, particle size

distribution, composition ratio). Furthermore, as non-spherical particles exist in ambient atmosphere, an estimate of the uncertainty induced by particle shape is needed before the optically effective ACRI being used to account for coarse composite aerosols in aerosol-climate models, which will hopefully be addressed in follow-up studies.

Acknowledgments

This work is financially supported by the National Natural Science Foundation of China (NSFC) (Nos. 41505127, 21406189), Natural Science Foundation of Jiangsu Province (No. BK20150901), and Key Laboratory of Meteorological Disaster of Ministry of Education (No. KLME201810). This work is also supported by the Key Laboratory of Middle Atmosphere and Global Environment Observation, Institute of Atmospheric Physics, Chinese Academy of Sciences (LAGEO-2019-04), and Startup Foundation for Introducing Talent of NUIST (Nos. 2015r002, 2014r011). Key Lab of Photovoltaic and Energy Conservation Materials, Chinese Academy of Sciences is gratefully acknowledged by the authors (PECL2019KF006). We acknowledge the source of the code of DDSCAT 7.3.

References

Abo Riziq, A., Erlick, C., Dinar, E., Rudich, Y., 2007. Optical properties of absorbing and non-absorbing aerosols retrieved by cavity ring down (CRD) spectroscopy. Atmos. Chem. Phys. 7, 1523–1536.

Alexander, J.M., Laskina, O., Meland, B., Young, M.A., Grassian, V.H., Kleiber, P.D., 2013. A combined laboratory and modeling study of the infrared extinction and visible light scattering properties of mineral dust aerosol. J. Geophys. Res. 118, 435–452.

Aouizerats, B., Thouron, O., Tulet, P., Mallet, M., Gomes, L., Henzing, J.S., 2010. Development of an online radiative module for the computation of aerosol optical properties in 3-D atmospheric models: validation during the EUCAARI campaign. Geosci. Model Dev. 3, 553–564.

Balkanski, Y., Schulz, M., Claquin, T., Guibert, S., 2007. Reevaluation of Mineral aerosol radiative forcings suggests a better agreement with satellite and AERONET data. Atmos. Chem. Phys. 7, 81–95.

Bellouin, N., 2014. The color of smoke. Nat. Geosci. 7, 619–629.

Bond, T.C., Bergstrom, R.W., 2006. Light absorption by carbonaceous particles: an investigative review. Aerosol Sci. Technol. 40, 27–67.

Bruggeman, D.A.G., 1935. Calculation of various physics constants in heterogeneous substances. I. Dielectricity constants and conductivity of mixed bodies from isotropic substances. Ann. Phys. 24, 636–664.

Cappa, C.D., Onasch, T.B., Massoli, P., Worsnop, D.R., Bates, T.S., Cross, E.S., Davidovits, P., Hakala, J., Hayden, K.L., Jobson, B.T., Kolesar, K.R., Lack, D.A., Lerner, B.M., Li, S., Mellon, D., Nuaaman, I., Olfert, J.S., Petaja, T., Quinn, P.K., Song, C., Subramanian, R., Williams, E.J., Zaveri, R.A., 2012. Radiative absorption enhancements due to the mixing state of atmospheric black carbon. Science 337, 1078–1081.

Chazette, P., Liousse, C., 2001. A case study of optical and chemical apportionment for urban aerosols in Thessaloniki. Atmos. Environ. 35, 2497–2506.

Draine, B.T., Flatau, P.J., 1994. Discrete-dipole approximation for scattering calculations. J. Opt. Soc. Am. 11, 1491–1499.

Draine, B.T., Flatau, P.J., 2008. Discrete dipole approximation for periodic targets: I. Theory and tests. J. Opt. Soc. Am. 25, 2693–2703.

Dubovik, O., Holben, B.N., Lapyonok, T., Sinyuk, A., Mishchenko, M.I., Yang, P., Slutsker, I., 2002. Non-spherical aerosol retrieval method employing light scattering by spheroids. Geophys. Res. Lett. 29, 1415.

Dubovik, O., Sinyuk, A., Lapyonok, T., Holben, B.N., Mishchenko, M., Yang, P., Eck, T.F., Volten, H., Munoz, O., Veihelmann, B., van der Zande, W.J., Leon, J.F., Sorokin, M., Slutsker, I., 2006. Application of spheroid models to account for aerosol particle nonsphericity in remote sensing of desert dust. J. Geophys. Res. 111, D11208.

Flatau, P.J., Draine, B.T., 2012. Fast near-field calculations in the discrete dipole approximation for regular rectilinear grids. Opt. Express 20 (2), 1247–1252.

Grieshop, A.P., Reynolds, C.C.O., Kandlikar, M., Dowlatabadi, H., 2009. A black-carbon mitigation wedge. Nat. Geosci. 2, 533.

Guazzotti, S.A., Coffee, K.R., Prather, K.A., 2001. Continuous measurements of size-resolved particle chemistry during INDOEX-Intensive Field Phase 99. J. Geophys. Res. 106, 28607–28628.

Guyon, P., Boucher, O., Graham, B., Beck, J., Mayol-Bracero, O.L., Roberts, G.C., Maenhaut, W., Artaxo, P., Andreae, M.O., 2003. Refractive index of aerosol particles over the Amazon tropical forest during LBA-EUSTACH 1999. J. Aerosol Sci. 34, 883–907.

Intergovernmental Panel on Climate Change (IPCC), 2003. Climate Change 2013: the Physical Science Basis. Cambridge University Press, UK.

Kandler, K., Schutz, L., Deutscher, C., Ebert, M., Hofmann, H., Jackel, S., Jaenicke, R., Knippertz, P., Lieke, K., Massling, A., Petzold, A., Schladitz, A., Weinzierl, B., Wiedensohler, A., Zorn, S., Weinbruch, S., 2009. Size distribution, mass concentration, chemical and mineralogical composition and derived optical parameters of the boundary layer aerosol at Tinfou, Morocco, during SAMUM 2006. Tellus B 61, 32–50.

Liu, S., Aiken, A.C., Gorkowski, K., Dubey, M.K., Cappa, C.D., Williams, L.R., Herndon, S. C., Massoli, P., Fortner, E.C., Chhabra, P.S., 2015. Enhanced light absorption by mixed source black and brown carbon particles in UK winter. Nat. Commun. 6, 8435.

Mack, L.A., Levin, E.J.T., Kreidenweis, S.M., Obrist, D., Moosmuller, H., Lewis, K.A., Arnott, W.P., McMeeking, G.R., Sullivan, A.P., Wold, C.E., Hao, W.M., Collett Jr., J. L., Malm, W.C., 2010. Optical closure experiments for biomass smoke aerosols. Atmos. Chem. Phys. 10, 9017–9026.

Marley, N.A., Gaffney, J.S., Baird, J.C., Blazer, C.A., Drayton, P.J., Frederick, J.E., 2001. An empirical method for the determination of the complex refractive index of size-fractionated atmospheric aerosols for radiative transfer calculations. Aerosol Sci. Technol. 34, 535–549.

Mishchenko, M.I., Dlugach, J.M., Liu, L., 2016. Applicability of the effective-medium approximation to heterogeneous aerosol particles. J. Quant. Spectrosc. Radiat. Transf. 178, 284–294.

Moteki, N., Kondo, Y., 2007. Effects of mixing state on black carbon measurement by laser-induced incandescence. Aerosol Sci. Technol. 41, 398–417.

Muller, D., Weinzierl, B., Petzold, A., Kandler, K., Ansmann, A., Muller, T., Tesche, M., Freudenthaler, V., Esselborn, M., Heese, B., Althausen, D., Schladitz, A., Otto, S., Knippertz, P., 2010. Mineral dust observed with AERONET Sun photometer, Raman lidar, and in situ instruments during SAMUM 2006: shape-independent particle properties. J. Geophys. Res. 115, D07202.

Muller, T., Schladitz, A., Massling, A., Kaaden, N., Kandler, K., Wiedensohler, A., 2009. Spectral absorption coefficients and imaginary parts of refractive indices of Saharan dust during SAMUM-1. Tellus B 61, 79–95.

Peng, J., Hua, M., Guo, S., Du, Z., Zheng, J., Shang, D., Zamora, M.L., Zeng, L., Shao, M., Wu, Y., Zheng, J., Wang, Y., Glen, C.R., Collins, D.R., Molina, M.J., Zhang, R., 2016. Markedly enhanced absorption and direct radiative forcing of black carbon under polluted urban environments. Proc. Natl. Acad. Sci. U.S.A. 113, 4266–4271.

Petzold, A., Rasp, K., Weinzierl, B., Esselborn, M., Hamburger, T., Dornbrack, A., Kandler, K., Schutz, L., Knippertz, P., Fiebig, M., Virkkula, A., 2009. Saharan dust absorption and refractive index from aircraft-based observations during SAMUM 2006. Tellus B 61, 118–130.

Raut, J.C., Chazette, P., 2008. Radiative budget in the presence of multi-layered aerosol. Atmos. Chem. Phys. 8, 6839–6864.

Raut, J.C., Chazette, P., 2008. Vertical profiles of urban aerosol complex refractive index in the frame of ESQUIF airborne measurements. Atmos. Chem. Phys. 8, 901–919.

Redemann, J., Turco, R.P., Liou, K.N., Russell, P.B., Bergstrom, R.W., Schmid, B., Livingston, J.M., Hobbs, P.V., Hartley, W.S., Ismail, S., Ferrare, R.A., Browell, E.V., 2000. Retrieving the vertical structure of the effective aerosol complex index of refraction from a combination of aerosol in situ and remote sensing measurements during TARFOX. J. Geophys. Res. 105 (D8), 9949–9970.

Roelofs, G.-J., ten Brink, H., Kiendler-Scharr, A., de Leeuw, G., Mensah, A., Minikin, A., Otjes, R., 2010. Evaluation of simulated aerosol properties with the aerosol-climate model ECHAM5-HAM using observations from the IMPACT field campaign. Atmos. Chem. Phys. 10, 7709–7722.

Riziq, A.A., Erlick, C., Dinar, E., Rudich, Y., 2007. Optical properties of absorbing and non-absorbing aerosols retrieved by cavity ring down (CRD) spectroscopy. Atmos. Chem. Phys. 7, 1523–1536.

Saija, R., Iati, M.A., Giusto, A., Borghese, F., Denti, P., Aiello, S., Cecchi-Pestellini, C., 2003. Radiation pressure cross-sections of fluffy interstellar grains. Mon. Not. R. Astron. Soc. 341, 1239–1245.

Saleh, R., Robinson, E.S., Tkacik, D.S., Ahern, A.T., Liu, S., Aiken, A.C., Sullivan, R.C., Presto, A.A., Dubey, M.K., Yokelson, R.J., Donahue, N.M., Robinson, A.L., 2014. Brownness of organics in aerosols from biomass burning linked to their black carbon content. Nat. Geosci. 7, 647–650.

Schkolnik, G., Chand, D., Hoffer, A., Andreae, M.O., Erlick, C., Swietlicki, E., Rudich, Y., 2007. Constraining the density and complex refractive index of elemental and organic carbon in biomass burning aerosol using optical and chemical measurements. Atmos. Environ. 41, 1107–1118.

Shi, C., Hashimoto, M., Nakajima, T., 2019. Remote sensing of aerosol properties from multi-wavelength and multi-pixel information over the ocean. Atmos. Chem. Phys. 19, 2461–2475.

Shindell, D., Kuylenstierna, J.C.I., Vignati, E., van Dingenen, R., Amann, M., Klimont, Z., Anenberg, S.C., Muller, N., Janssens-Maenhout, G., Raes, F., Schwartz, J., Faluvegi, G., Pozzoli, L., Kupiainen, K., Hoglund-Isaksson, L., Emberson, L., Streets, D., Ramanathan, V., Hicks, K., Oanh, N.T.K., Milly, G., Williams, M., Demkine, V., Fowler, D., 2012. Simultaneously mitigating near-term climate change and improving human health and food security. Science 335, 183.

Shiraiwa, M., Kondo, Y., Moteki, N., Takegawa, N., Miyazaki, Y., Blake, D.R., 2007. Evolution of mixing state of black carbon in polluted air from Tokyo. Geophys. Res. Lett. 34, L16803.

Smith, A.J.A., Grainger, R.G., 2014. Simplifying the calculation of light scattering properties for black carbon fractal aggregates. Atmos. Chem. Phys. 14 (15), 7825–7836.

Stier, P., Feichter, J., Kinne, S., Kloster, S., Vignati, E., Wilson, J., Ganzeveld, L., Tegen, I., Werner, M., Balkanski, Y., Schulz, M., Boucher, O., Minikin, A., Petzold, A., 2005. The aerosol-climate model ECHAM5-HAM. Atmos. Chem. Phys. 5, 1125–1156.

Stock, M., Cheng, Y.F., Birmili, W., Massling, A., Wehner, B., Muller, T., Leinert, S., Kalivitis, N., Mihalopoulos, N., Wiedensohler, A., 2011. Hygroscopic properties of atmospheric aerosol particles over the Eastern Mediterranean: implications for regional direct radiative forcing under clean and polluted conditions. Atmos. Chem. Phys. 11, 4251–4271.

Voshchinnikov, N.V., Videen, G., Henning, T., 2007. Effective medium theories for irregular fluffy structures: aggregation of small particles. Appl. Opt. 46 (19), 4065–4072.
Wiscombe, W.J., 1980. Improved Mie scattering algorithm. Appl. Opt. 19 (9), 1505–1509.
Zhang, X., Huang, Y., Rao, R., Wang, Z., 2013. Retrieval of effective complex refractive index from intensive measurements of characteristics of ambient aerosols in the boundary layer. Opt. Express 21 (15), 17849–17862.
Zhang, X., Mao, M., Yin, Y., Wang, B., 2017. Absorption enhancement of aged black carbon aerosols affected by their microphysics: a numerical investigation. J. Quant. Spectrosc. Radiat. Transf. 202, 90–97.
Zhang, X., Mao, M., Yin, Y., Wang, B., 2018. Numerical investigation on absorption enhancement of black carbon aerosols partially coated with nonabsorbing organics. J. Geophys. Res. 123, 1297–1308.